Andrew Shansby
April 11, 2006

Comparison of the Petrology of Samples from Two Amphibolite Facies Localities from the Andrelândia Group, Brazil

A Geology 394 Senior Thesis Project
Supervisors: Drs. Michael Brown and Phil Piccoli, and PhD student Barry Reno

Abstract

This is a study of the possible melting of a biotite schist unit in the Andrelândia Group, Minas Gerais, Brazil, through the use of petrology and apatite chemistry. The Andrelândia Group comprises a system of nappes metamorphosed at greenschist to high pressure granulite facies. Within this group, the Andrelândia Nappe comprises an amphibolite facies metapelitic unit, consisting primarily of a biotite schist. The study involves samples from this nappe from two quarries near Cambuquira, Minas Gerais. In the INCOPE quarry, melt may have been generated during metamorphism, as reflected by the presence of extensive feldspar-bearing leucosome in biotite-garnet gneiss. At the abandoned quarry, monomineralic quartz veins in a biotite-garnet schist indicate melting did not occur, because the melting temperature of monomineralic quartz is too high. Previous studies by Kapustin have suggested that the composition of apatite may reflect metamorphic grade. Apatite from samples in both quarries were analyzed for F, Cl, and OH in order to understand the effect of increasing metamorphic grade on apatite chemistry. There is no significant difference between apatite composition at the two localities, which may suggest that melting has not occurred.

Introduction

In metamorphic rocks, apatite composition can yield information about the geologic history of the rock (Spear and Pyle, 2002). The chemical composition of apatite within the samples may reflect changes that occur relating to metamorphism and melting, and whether water was involved with any possible partial melting. Kapustin (1987) studied the chemistry of apatite across a large metamorphic gradient, and suggests that there is a regular change in chemistry with changing pressure and temperature conditions. Kapustin (1987) suggested that F, Cl and OH change systematically with increasing metamorphic grade. In the study, Kapustin looked at apatite in a wide variety of rock types (e.g. pelites, carbonates), and found the F concentration of apatite to increase from the greenschist to granulite facies (Figure 1).

Geology and Geologic Setting

The Neoproterozoic Brasilia Fold Belt (BFB) (Figure 2) lies between the São Francisco Craton (SFC), the Amazonas Craton and the Paranapanema Craton in central Brazil (Campos Neto, 2000). The BFB is a fold and thrust belt that extends in the north – south direction along the western edge of the SFC (Campos Neto, 2000). During the Neoproterozoic, sediments were deposited off shore from the SFC along a passive margin setting into the Brazilides Ocean, between the SFC, and Amazonas and Paranapanema Cratons. The São Francisco Plate, which includes the SFC in addition to western Brazilides Ocean floor began to subduct under the Amazonas and the Panapanema Plates at 900 - 850 Ma (Junges et al., 2002). The subducting SFC released fluid, lowering the melting point for the overlying mantle. Magma was generated during subduction of the São Francisco Plate leading to the formation of the intra-oceanic Goiás Magmatic Arc (GMA) (Campos Neto and Caby, 1999). Sediments from both the SFC and the newly formed GMA continued to accumulate in the Brazilides Ocean. The GMA migrated to the east. As subduction of the São Francisco Plate continued, the GMA collided with the SFC. Sediments in the Brazilides Ocean accreted to the western edge of the SFC. The Amazonas and Paranapanema Cratons collided with the GMA, the sediments, and the SFC, resulting in deformation and metamorphism of these units.

In the southern BFB, this deformation and metamorphism resulted in the nappe structure exposed today on the southern edge of the SFC (Campos Neto and Caby, 1999). The nappe structure consists of the lower portion of the GMA overlying a series of nappes comprised of Brazilides Oceanic metasedimentary and related rocks which in turn, lie on top of the SFC (Figure 3). The nappes decrease in peak metamorphic temperature to the base of the group (Garcia et al., 2003b). The upper Soccorro-Guaxupé Nappe is a sub-horizontal to southwest dipping high-temperature granulite-migmatitic allochthon (Campos Neto and Caby, 2000). The Três Pontas-Varginha nappe, immediately below the Soccorro-Guaxupé Nappe, comprises of a 5 km thick unit of high pressure kyanite-granulites. Beneath the Três Pontas-Varginha nappe is the Andrelândia nappe, which includes the two quarries of interest for this paper (Figure 4). The Andrelândia nappe is comprised of a metapelitic lithofacies that is present throughout the Andrelândia Group. This nappe was subjected to amphibolite facies metamorphism at ca. 640 Ma (Reno, Pers. Comm.) and primarily comprises a garnet mica-schist in the southern portion of the nappe, and a garnet-biotite-plagioclase gneiss in the northern portion of the nappe. This unit lies over a quartzite nappe composed predominantly of passive continental margin sediments, which, in turn, is on top of the Parautochthonous nappe overlying the SFC at the southern edge of the SFC. Peak metamorphism of the group occurred due to the continental collision, and ocean basin closure (Campos Neto and Caby, 1999).

Field area

The field area of study consists of two quarries, 15 km apart, in between which is the town of Cambuquira (Figure 4). The quarry south of Cambuquira is abandoned, whereas the quarry north of Cambuquira is the INCOPE Ltda. working quarry.

Rock samples

Three samples of biotite-garnet schist were collected from the abandoned quarry (GR-05-01, GR-05-02, and 04-5-2). Sample GR-05-01 is a quartz vein rich sample comprised of (based upon visual approximations and in hand specimine), quartz veins, garnet which has a maximum observed diameter of 5 mm, and dark biotite rich bands. Sample GR-05-02 is a quartz vein poor sample, comprising of quartz veins, garnet which has a maximum observed diameter of 3 mm, and dark bands with biotite (60%). Sample 04-5-2 (Figure 6), which is similar to GR-05-02, was chosen for apatite analysis because it is the most biotite-rich sample. **Apatite was most often found bordering or contained within biotite and garnet.** Thin section petrography of each of the 04 samples reveal quartz (30%), biotite (20%) up to 2 mm in diameter, garnet (15%) with inclusions of quartz, biotite, and apatite (2%), muscovite (10%) up to 5 mm in diameter, kyanite (5%), tourmaline (2%), the largest is 2 mm, apatite (2%) within the garnet, plagioclase (15%), and chlorite replacing biotite (3%).

Three samples were collected from the INCOPE quarry (GR-05-03, GR-05-04, and 04-5-5). Sample GR-05-03 contains leucosome (60%), with the largest segregations measuring 1 cm. The remainder of the sample comprises biotite (25%) and garnets (15%) of up to 5 mm. Sample GR-05-04 contains 30% quartz-plagioclase leucosome, with the largest segregations measuring 3 mm. Garnet (10%) reaches 5 mm in diameter. The rest of the sample comprises dark bands of biotite and plagioclase. Sample 04-5-5 (Figure 7), which is similar to GR-05-03, was also chosen for apatite analysis. It comprises veins (50%), with approximately equal proportions quartz and plagioclase, bands of foliated biotite (20%) up to 3 mm long, garnet (15%). Garnet often contains inclusions of biotite, quartz, and chlorite. Muscovite (5%) is commonly between biotite layers, reaching up to 1 cm in length. Apatite (2%) is found in plagioclase, garnet and biotite, kyanite (3%) is found as inclusions in muscovite and garnet.

Phosphate Chemistry

Apatite, a calcium phosphate that is commonly found in metamorphic rocks, contains trace amounts of LREE and HREE. The halogen site substitution in apatite is the focus of study. In apatite, $Ca_5(PO_4)_3(F,Cl,OH)$, the halogen site (F,Cl,OH) is usually full, and, for this study, vacancies are assumed not to exist, and each halogen site is assumed to be filled by F, Cl, or OH only. A carbon or oxygen ion may rarely occupy the halogen site, however this is rare occurrence (Piccoli and Candela, 2002) and for the purposes here will be ignored

Using WDS, one can measure F and Cl concentrations to calculate the concentrations of the flourapatite and chlorapatite, respectively, components in apatite. The component of flourapatite in apatite is

$$\text{FAp}\,\% = \left(\frac{\text{wt.}\,\%\,\text{F}}{3.767}\right) * 100\% \qquad (1)$$

and the component of chlorapatite in apatite is

$$\text{CAp}\,\% = \left(\frac{\text{wt.}\,\%\,\text{Cl}}{6.81}\right) * 100\% \qquad (2)$$

With FAp and CAp calculated, hydroxylapatite (HAp) can then be calculated using the equation

$$\text{HAp}\,\% = 100 - \text{FAp} - \text{CAp} \qquad (3)$$

by inputting the values from equations (1) and (2).

Statement of Problem

The INCOPE quarry biotite gneiss potentially experienced partial melting during metamorphism suggested by plagioclase and quartz bearing leucosomes. Plagioclase - quartz bearing leucosomes imply the leucosome could have crystallized from a granitic liquid. Monomineralic quartz is not likely to have been a melt because the melting temperature for monomineralic quartz is too high. The biotite schist at the abandoned quarry most likely did not experience melting as it only contains quartz veins without plagioclase. Determining whether partial melting occurred in the rocks from either quarry will be a focus of the study. If partial melting did occur, there is the question of whether the melting was due to mica breakdown or caused by an influx of water. Apatite composition may to be influenced by metamorphic grade (Figure 1). According to the Kapustin study, apatite in lower grade metamorphic rocks has a greater CAp component and HAp component. Apatite in higher grade metamorphic rocks may have more of a FAp component. This project explores whether apatite chemistry will relate to the melting history of a rock.

Hypothesis

The rocks from the INCOPE quarry experienced partial melting whereas the rocks from the abandoned quarry locality did not experience partial melting. Apatite chemistry will reflect the occurrence of partial melting, and will reflect the metamorphic grade.

Limitations

Whereas pressure and temperature conditions have been calculated for the Andrelândia nappe, peak pressures and temperatures for rocks from these two quarries have not been calculated. The samples are from a large area mapped as one lithotectonic unit, so the rocks are assumed to have the same protolith. Even though they are similar in composition, the two quarries are separated by 15 km, so the protolith composition could vary slightly with distance.

Methods

Samples from both quarries were collected in 2004 by Reno, and in 2005 by Reno and Shansby.

Tools used for the analysis of the samples include a rock saw, a hand lens, a petrographic microscope, and an electron probe microanalyzer (EPMA). A rock saw was used to cut centimeter-thick slabs from the sample rocks. The slabs were sent to Spectrum Petrographics, Inc. in Vancouver, WA, for thin section preparation. A hand lens and petrographic microscope were used to identify the mineralogy of each of the samples. The mineralogy, relationship between minerals, their distribution, grain size, shape, and any replacement minerals for each of the samples were recorded, and differences in each of these categories between samples were noted. A digital camera, attached to a petrographic microscope, was used to document microstructures in the thin sections.

A flat-bed scanner was used to capture an image of entire thin sections to map for apatite. Apatite grains were marked on a full-page scan of the thin section for further analysis in the EPMA (Figure 8), and the phases with which it is associated with were recorded. Approximately 20 apatite grains were located in each of the samples. Backscatter electron images (BSE) were taken of each apatite grain (Figure 9).

Two types of analyses can be performed on the EPMA: energy dispersive spectroscopy (EDS), and wavelength dispersive spectroscopy (WDS). EDS can detect major and minor elements with atomic number greater than seven (boron), and measure concentrations above approximately 1000 ppm (this value is dependant on the element) for a chosen field of view. WDS uses a focusing spectrometer which returns an accurate and precise amount of one element. The analytical protocol was modified to reduce the detection limits of select elements (e.g. Cl, Fe). This was accomplished by increasing the count time (for example, up to 240 seconds total count time for Cl). For these analyses, the minimum detection limit was approximately 30 ppm for Cl. The apatite was analyzed as a function of petrographic relationship, that is the location of the point within the grain (core / rim), and the phase containing the grain.

In each of the apatite grains, points were selected for WDS analysis to obtain elemental concentrations. For small grains (those on the order of 10 μm), one point was analyzed in the center of the apatite grain. In the larger grains (those on the order of 100 μm), three to seven points were analyzed. Apatite grains were chosen in a variety of associations. For example, apatite was located within the garnet, bordering biotite, and plagioclase, and bordering different combinations of minerals. On the EPMA, WDS was used to determine the concentrations in apatite of F, Ca, Cl, P, Fe, Mn, Sr, Mg, La, Ce, Si, and S for each point.

Data were analyzed in a rigorous statistical fashion. Error was assessed using standard errors due to x-ray counting statistics and standard error propagation procedures. The calculations were made for the concentration and uncertainty from representative apatite grains for each of the two quarries. The chemical composition of the apatite from the samples were compared.

Results

Mineral Chemistry Results

Table 1 shows the mineral chemistry of each of the apatite grains measured in this study. A ternary diagram (Figure 10) reveals a low Cl concentration in each of the apatite grains. The average apatite composition from the two quarries are not significantly different. The Cl concentrations in apatite do not appear to have a correlation with which quarry the apatite is located (Figure 11). Neighboring or surrounding phases such as biotite or garnet do not influence the apatite composition (Table 1).

Outliers, data points with exceptionally high CAp components represent apatite inclusions in the core of garnet, such as Grain #1 of GR-05-3, and Grain #2 of GR-05-4A (Figure 11).

There is a wide range of F concentrations in apatite, and it appears to be zoned, as a greater F concentration is found on the rim of the apatite grains than in the core.

Analysis

The compositions of the samples are compared with other studies involving the behavior of apatite within metamorphic rocks, such as the results from studies by Kapustin (1987). Comparing Figures 1 and 10, the apatite compositions with this project have a similar range to the amphibolite apatite compositions in the Kapustin study, but there are some differences. The apatite in this study has a greater range of FAp values, and a more restricted range of CAp values. Since the rocks from this study are expected to have undergone similar metamorphism, and are part of the same metamorphic unit, this could cast doubts on the Kapustin data, as the average range of FAp values from this study is not represented on Kapustin's plot.

Zoning in the apatite grain could be a result of growth zoning while the melt was being crystallized. In the garnet, a slow diffusivity leads to the outer core having a different composition than the reaction rim (Spear and Pyle, 2002).

Conclusion

The hypothesis was that the INCOPE quarry rocks experienced partial melting. While the petrology of the rocks from INCOPE is consistent with melting and the petrology of the rocks from the abandoned quarry is consistent with melting not having occurred, the results remain inconclusive. Rocks from INCOPE are gneiss, have larger garnets, and a leucosome mineralogy consistent with melting. Rocks from the abandoned quarry are schist, have smaller grains, and veins that were not likely melted. The apatite composition is not significantly different, either in bordering different phases or in different rocks or in different quarries, suggesting that apatite composition is not indicative of a partial melt, or that melting did not occur. No demonstrative evidence of melting was found.

Works Cited

Bose, Sankar; Das, Kaushik; Fukuoka, Masato. Fluorine content of biotite in granulite-grade metapelitic assemblages and its implications for the Eastern Ghats granulites. European Journal of Mineralogy, Volume 17, Number 5, October 2005, pp. 665-674(10)

Campos Neto, M.C., 2000. Orogenic Systems From Southwestern Gondwana / An approach to Brasiliano-Pan African cycle and orogenic collage in Southeastern Brazil. Tectonic Evolution of South America, 335 – 365.

Campos Neto, M.C., Caby, R., 1999. Neoproterozoic high-pressure metamorphism and tectonic constraint from the nappe system south of the São Francisco Craton, Southeast Brazil. Precambrian Research 97, 3 – 26.

Campos Neto, M.C., Caby, R., 2000. Terrane accretion and upward extrusion of high-pressure granulites in the Neoproterozoic nappes of southeast Brazil: Petrologic and structural constraints. Tectonics 19 (4), 669 – 687.

Garcia, Maria da Glória M., Campos Neto, M.C., Fallick, A. E., 2003 (a). Contrasting metamorphic conditions in the Neoproterozoic collision-related Nappes south of São Francisco Craton, SE Brazil. Journal of South American Earth Sciences 15 (8), 853 – 870.

Garcia, Maria da Glória M., Campos Neto, M.C., Fallick, A. E., 2003 (b). Oxygen isotope composition and geothermometry of granulite to greenschist facies metamorphic rocks: a study from the Neoproterozoic collision-related nappe system, south of São Francisco Craton, SE Brazil. Journal of South American Earth Sciences 15 (8), 871 – 883.

Junges, L.S., Pimintel, M.M., and Moraes, R.d., 2002. Nd isotopic study of the Neoproterozoic Mara Rosa Arc Brazil: implications for the evolution of the Brazilia Belt. Precambrian Research 117, 101 – 118.

Kapustin, Yu. L., 1987. The composition of apatite from metamorphic rocks. Geochemistry International 24 (4), 45 – 51.

Piccoli, P.M. and Candela, P.A. 2002. Apatite in Igneous Systems. Phosphates-Geochemical, Geobiological, and Materials Importance, Kohn, M.J., Rakovan, J. and Hughes, J.M. (eds.). Reviews in Mineralogy and Geochemistry, 48, 255-292.

Santos, L.P., Campos Neto, M.C., and Grohmann, C.H 2004. Metamorphic path constrained by metapelitic rocks from the inner Aiuruoca- Andrelândia nappe, south of the São Francisco craton, SE Brazil. Journal of South American Earth Sciences 16, p. 725-741.

Spear, F.S., and Pyle, J.M. 2002. Apatite, monazite, and xenotime in metamorphic rocks. In M.J. Kohn, J. Rakovan, and J.M. Hughes, Eds. Phosphates: Geochemical, Geobiological, and Materials Importance, 48, p. 293-335. Reviews in Mineralogy and Geochemistry, Mineralogical Society of America, Washington, D. C.

Trouw, R.A.J.; Ribiero, A.; Paciullo, F.V.P. and Heilbron, M., 2000. Interference between the Neoproterozoic Brasília and Ribeira Belts, with Special Emphasis on High Pressure Granulites. Pre-Congress Field Trip. 31st International Geological Congress, Rio de Janeiro, Brazil, August 6 – 17, 2000, Field Trip Bft 08, 45p.

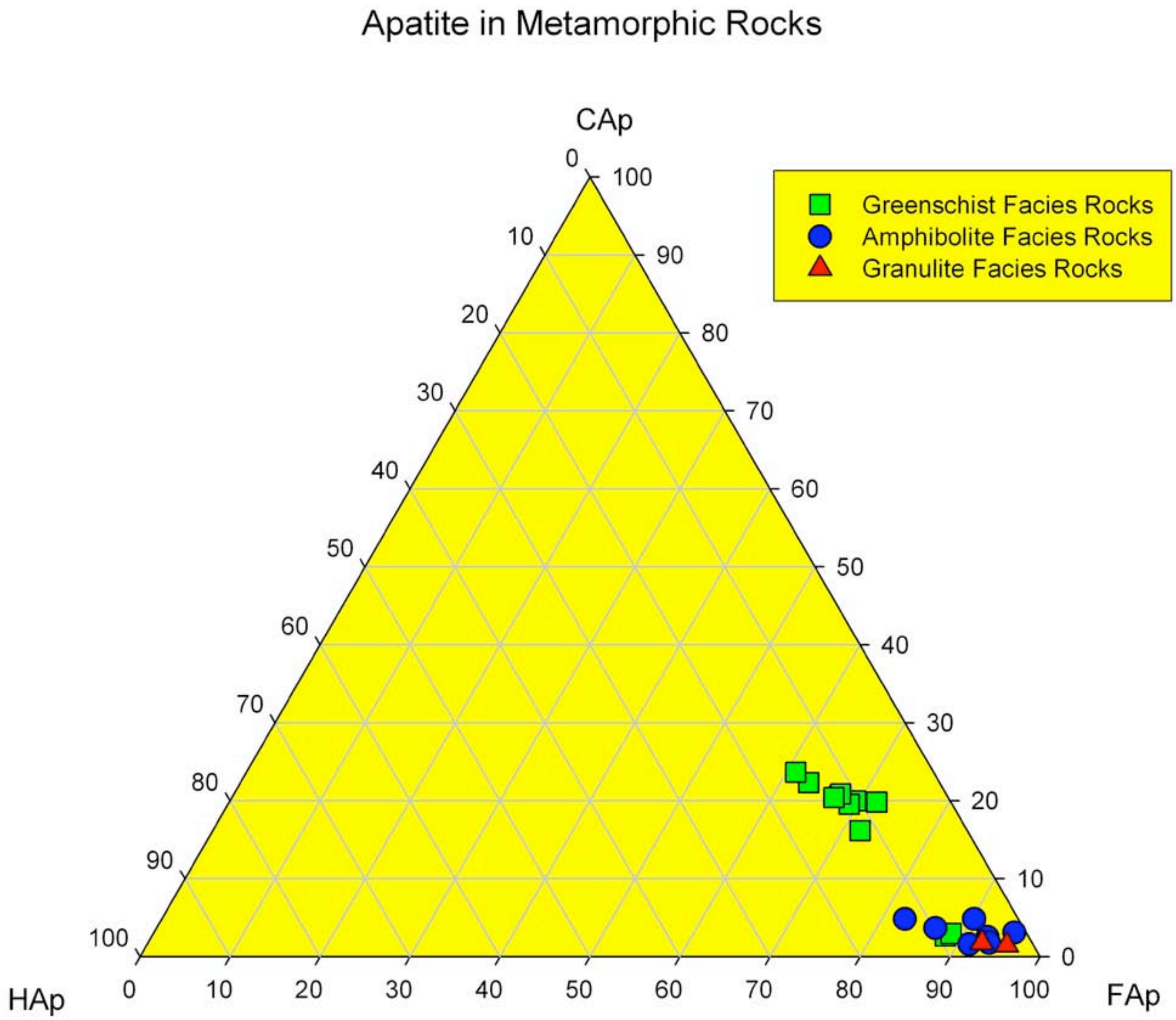

Figure 1: Proportions of chlorapatite, hydroxylapatite, and flourapatite based upon metamorphic grade (modified from Kapustin, 1987).

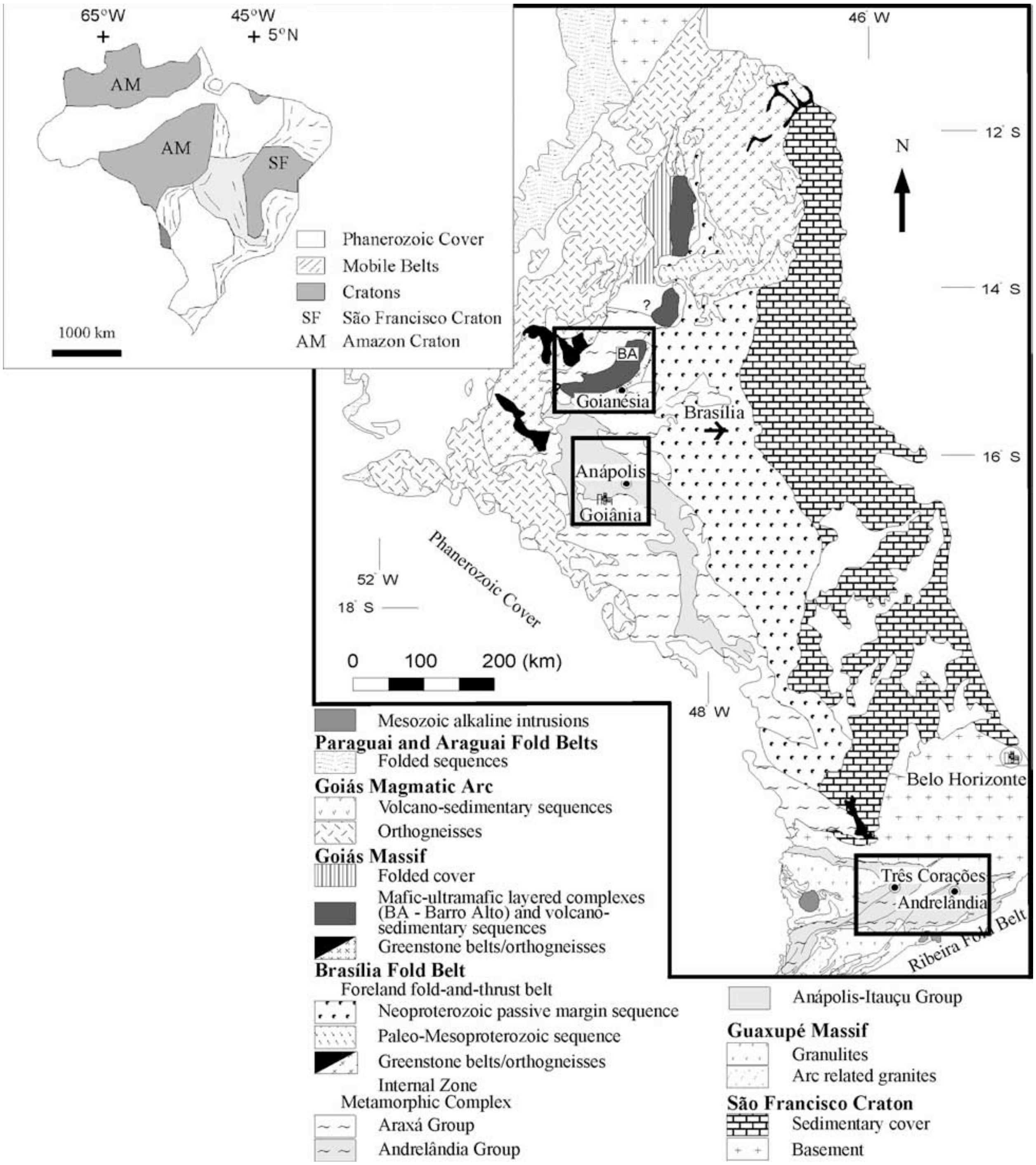

Figure 2: Brasília Fold Belt Geologic Map. The Andrelândia Group is in the box in the lower right of the right Figure.
(Brown, Pers. comm))

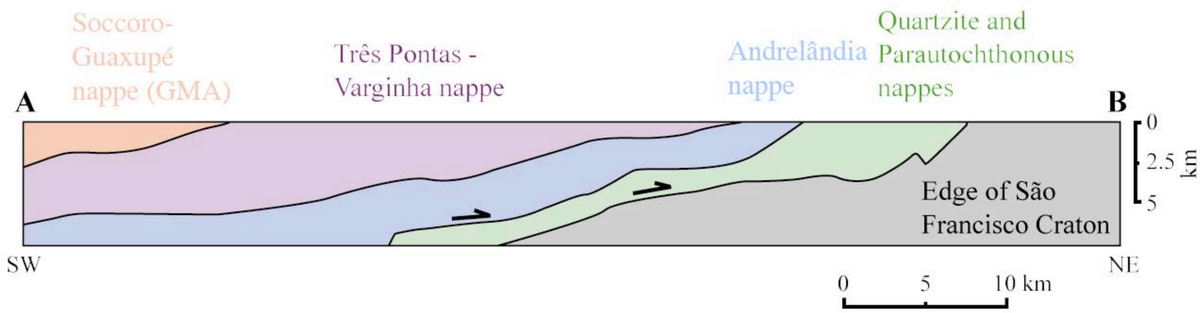

Figure 3: Cross section of nappes. See Figure 5 for cross section location. Modified from Campos Neto and Caby, 1999.

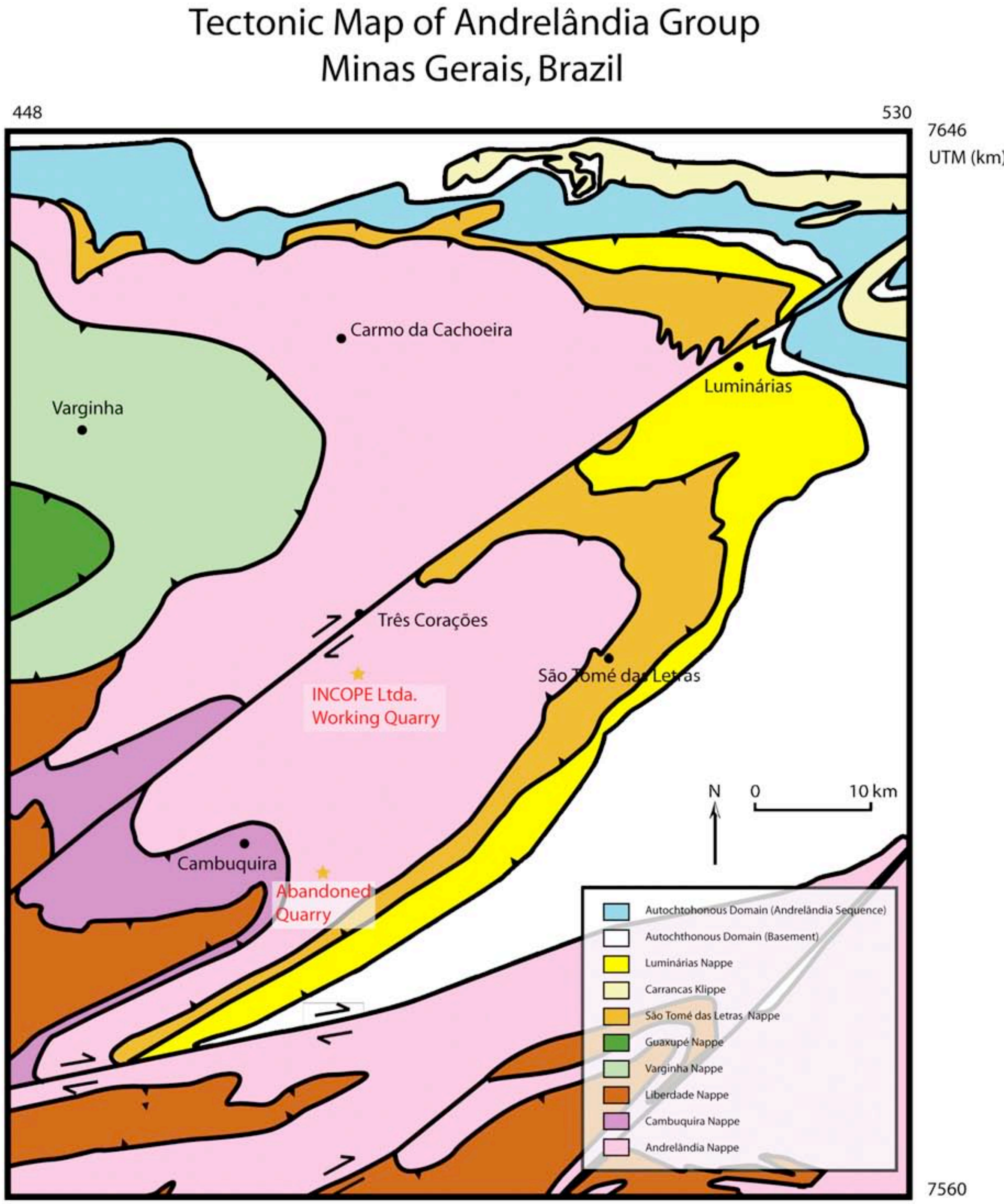

Figure 4: Tectonic map of southern Minas Gerais state, Brazil (After Trouw et al., 2003)

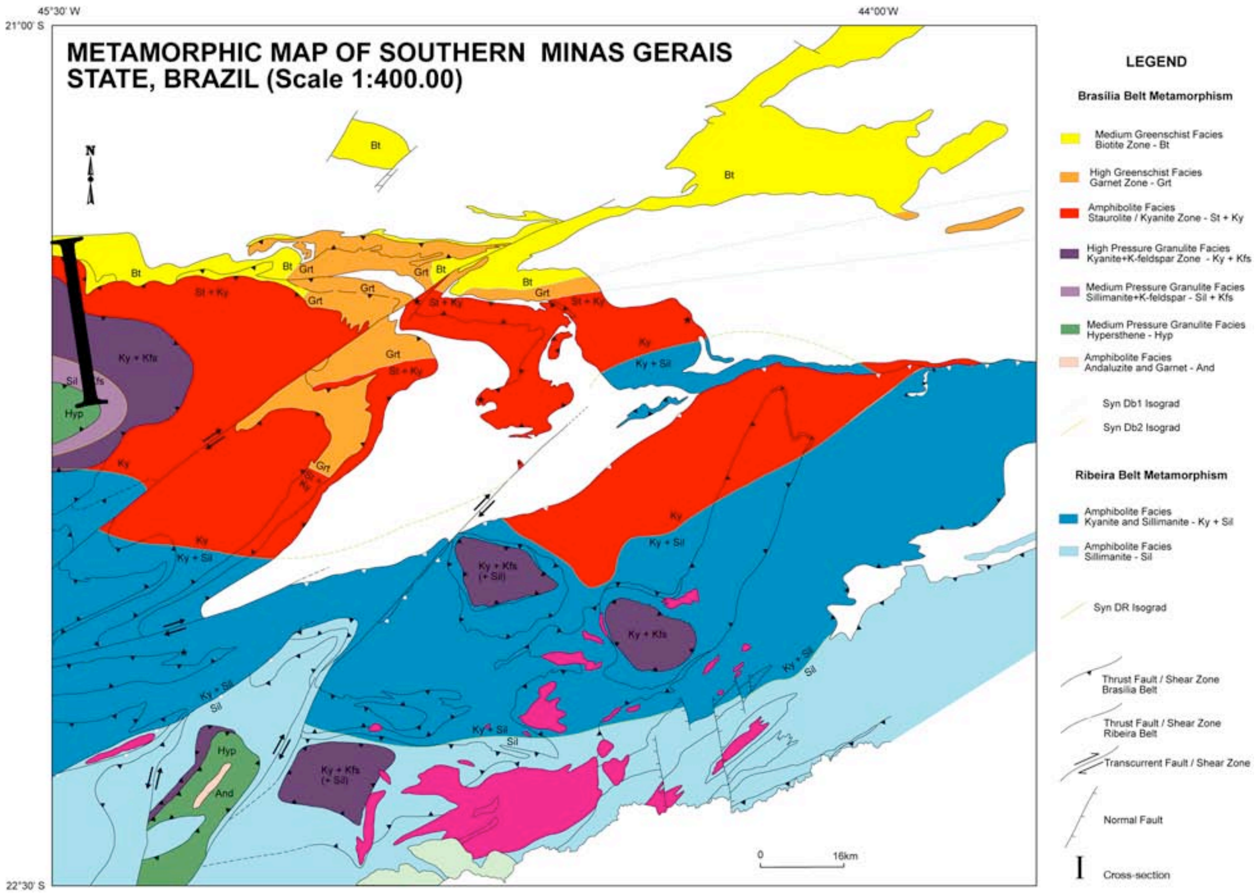

Figure 5: Metamorphic map of Southern Minas Gerais State, Brazil (Trouw, Pers. Comm)

I---I 2.5 cm

Figure 6: 04-5-2 thin section scan (Abandoned quarry)

Figure 7: 04-5-5 thin section scan (INCOPE quarry)

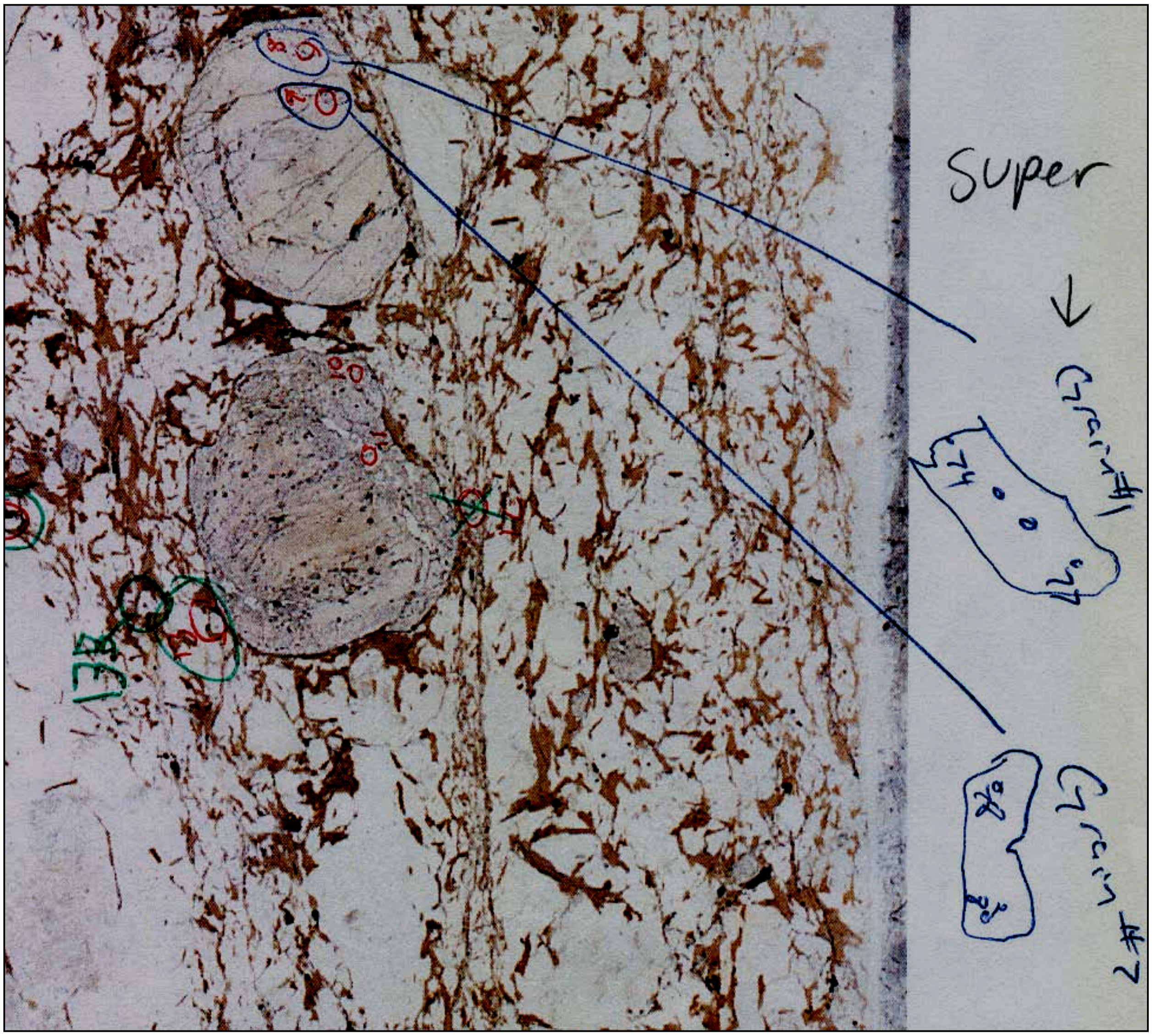

Figure 7: Apatite analysis map

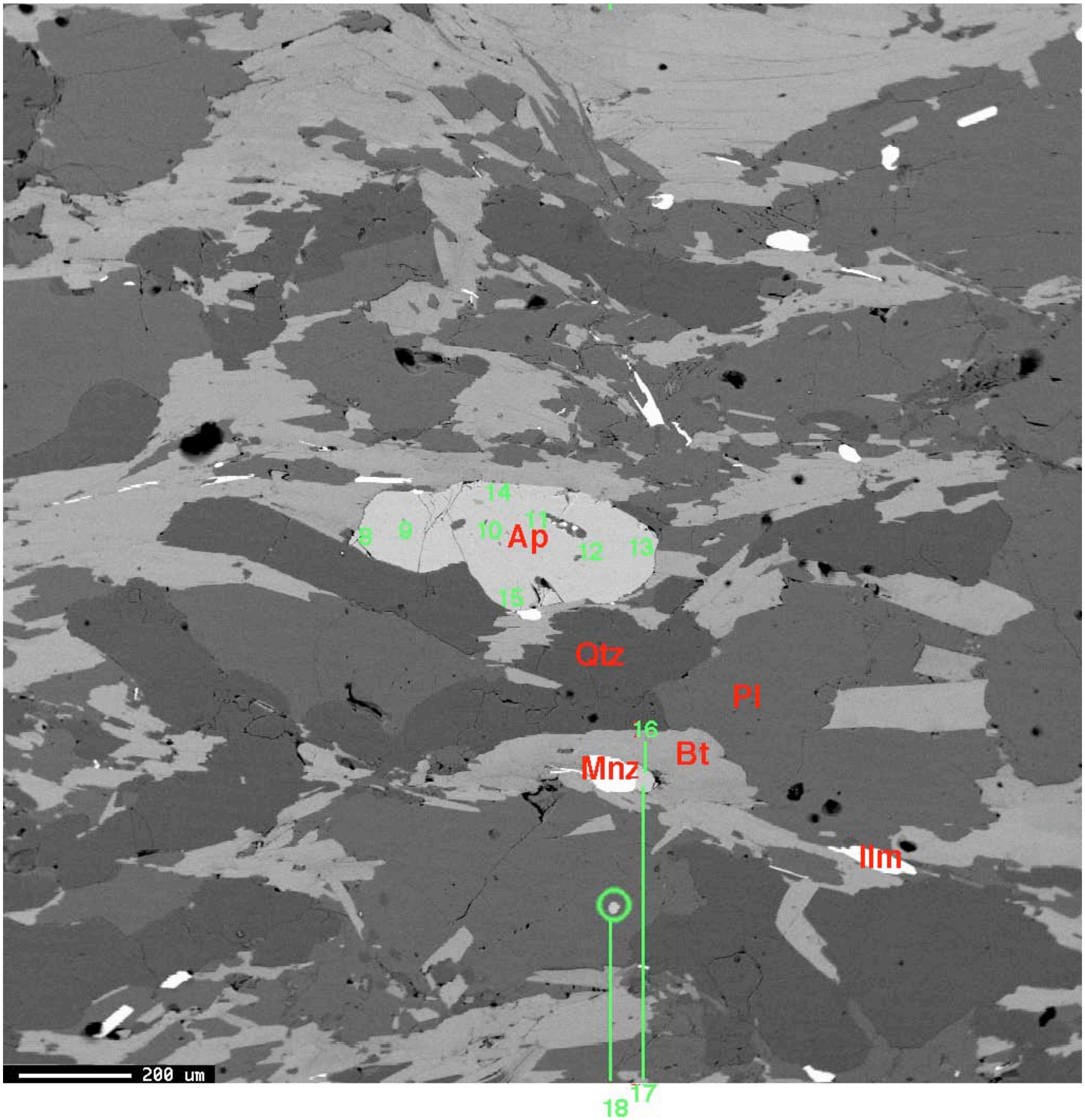

Figure 9: Backscatter electron image (BSE) of sample 04-5-2 (abandoned quarry). Apatite analysis points 8 – 18 and mineral phases labeled.

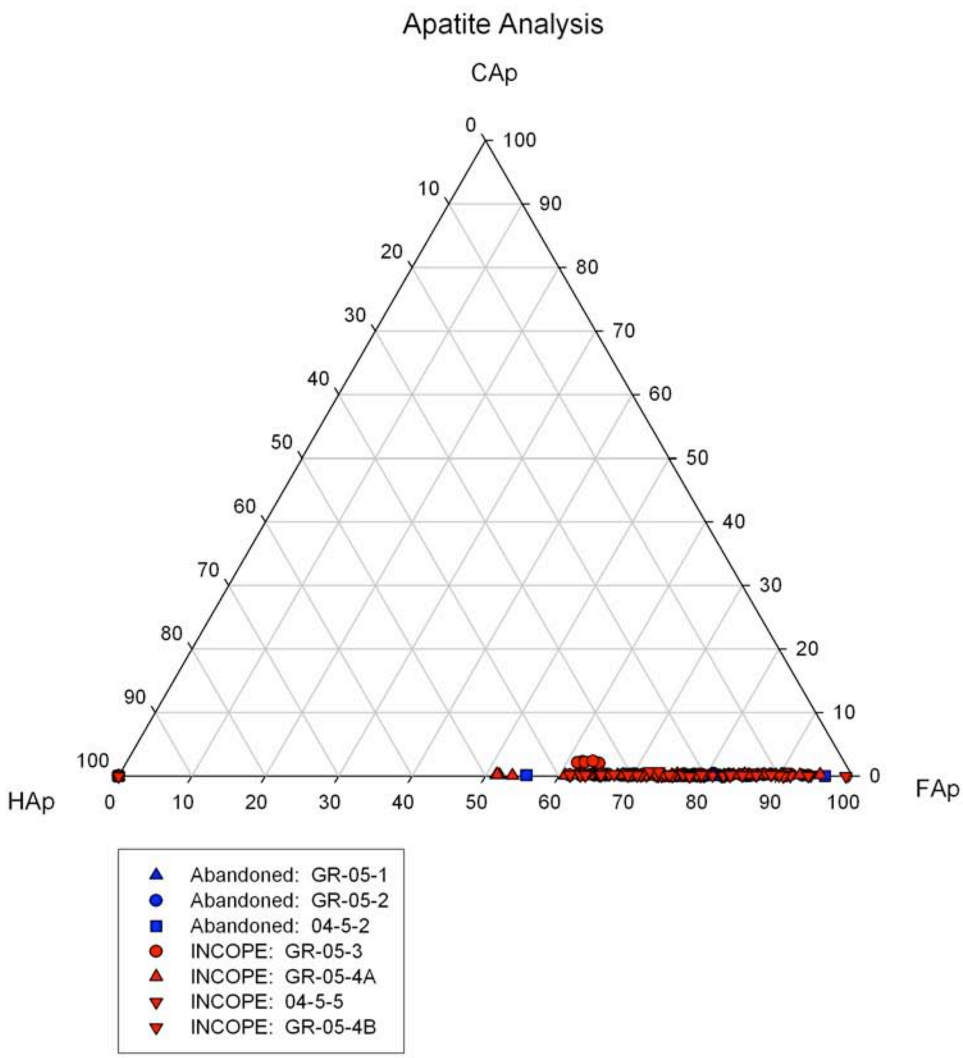

Figure 10: Plot of molar proportion chlorapatite [CAp], flourapatite [FAp], and hydroxylapatite [HAp] for data in Table 1.

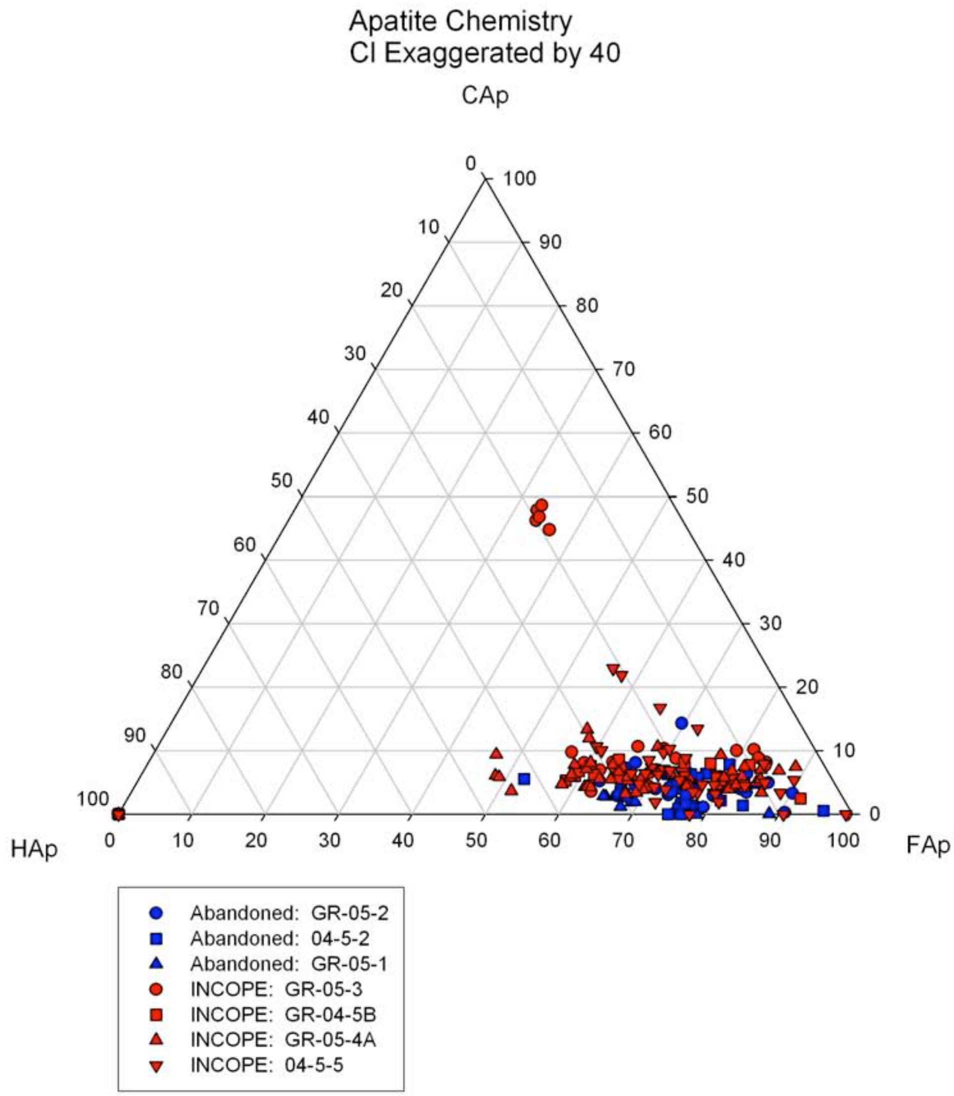

Figure 11: Plot of molar proportion chlorapatite [CAp] exaggerated by 40, flourapatite [FAp], and hydroxylapatite [HAp] for data in Table 1.

CaO	P2O5	Cl	F	FeO	MnO	total	Comment	phase	
wt %	wt %	wt %	wt %	wt %	wt %	wt %			
							Abandoned		
53.85	41.84	0.007	2.92	bd	bd	98.94	GR-05-02 (Grain#1)	bt, qtz	
53.50	41.82	0.007	2.99	bd	0.06	98.46	GR-05-02 (Grain#1)	bt, qtz	
54.52	41.54	bd	2.97	bd	bd	99.23	GR-05-02 (Grain#1)	bt, qtz	
53.66	42.20	0.006	2.61	0.03	bd	98.58	GR-05-02 (Grain#1)	bt, qtz	
53.44	42.20	0.003	2.90	bd	0.06	98.61	GR-05-02 (Grain #2)	bt, qtz	
53.46	42.30	0.007	3.24	bd	bd	99.07	GR-05-02 (Grain #2)	bt, qtz	
53.29	41.98	bd	2.86	bd	bd	98.26	GR-05-02 (Grain #2)	bt, qtz	
53.66	41.46	bd	3.01	bd	0.03	98.34	GR-05-02 (Grain #3)	bt, qtz	
54.44	42.32	0.005	2.85	0.04	0.04	99.88	GR-05-02 (Grain #3)	bt, qtz	
55.54	43.09	0.010	2.96	0.05	0.03	101.76	GR-05-02 (Grain #3)	bt, qtz	
54.94	42.23	0.011	3.31	bd	0.05	100.73	GR-05-02 (Grain #3)	bt, qtz	
53.92	42.31	0.007	2.79	bd	0.03	99.09	GR-05-02 (Grain #4)	bt, qtz	
54.54	42.26	bd	3.42	bd	bd	100.40	GR-05-02 (Grain #4)	bt, qtz	
54.36	41.86	0.006	3.27	bd	0.06	99.61	GR-05-02 (Grain #4)	bt, qtz	
54.53	41.97	0.005	3.09	bd	bd	99.77	GR-05-02 (Grain #4)	bt, qtz	
54.86	41.78	0.009	3.41	bd	0.03	100.24	GR-05-02 (Grain #4)	bt, qtz	
54.17	42.27	0.028	3.05	0.06	0.07	99.79	GR-05-02 (Grain #5)		
53.96	42.10	0.012	2.99	bd	0.12	99.34	GR-05-02 (Grain #5)		
53.82	42.17	0.007	3.13	bd	0.04	99.41	GR-05-02 (Grain #5)		
52.97	42.15	0.013	2.65	bd	bd	97.80	GR-05-02 (Grain #6)	bt, qtz, plag	
53.09	42.06	0.012	2.62	0.03	bd	97.83	GR-05-02 (Grain #6)	bt, qtz, plag	
53.25	41.72	0.005	2.58	bd	bd	97.64	GR-05-02 (Grain #6)	bt, qtz, plag	
52.62	41.60	0.007	2.61	bd	0.06	97.06	GR-05-02 (Grain #6)	bt, qtz, plag	
55.76	42.37	0.010	2.09	0.66	0.03	100.04	04-5-2 Grain #1 Rim (in Grt)	gt	
55.06	42.23	0.004	2.65	0.39	0.04	99.26	04-5-2 Grain #1 Core (in Grt)	gt	
56.05	43.13	0.011	2.87	0.40	0.03	101.29	04-5-2 Grain #1 Rim (in Grt)	gt	
55.63	43.00	0.012	3.09	0.64	0.07	101.14	04-5-2 Grain #2 Rim (in Grt)	gt	
54.59	41.81	0.009	2.91	0.52	0.03	98.65	04-5-2 Grain #2 Core (in Grt)	gt	
55.50	43.05	0.010	3.03	0.40	0.04	100.76	04-5-2 Grain #2 Core (in Grt)	gt	
54.46	42.25	0.015	3.24	0.72	0.07	99.39	04-5-2 Grain #2 Rim (in Grt)	gt	
54.60	42.19	0.011	3.00	0.08	0.04	98.66	04-5-2 Grain #3 (see image for location		
55.74	42.32	0.006	2.87	0.15	0.11	99.98	04-5-2 Grain #3 (see image for location		
54.87	41.82	bd	2.88	0.04	0.07	98.47	04-5-2 Grain #3 (see image for location		
54.71	42.14	bd	2.96	bd	0.09	98.65	04-5-2 Grain #3 (see image for location		

CaO	P2O5	Cl	F	FeO	MnO	total	Comment	phase	
wt %	wt %	wt %	wt %	wt %	wt %	wt %			
54.80	42.09	0.003	2.93	0.14	0.03	98.76	04-5-2 Grain #3 (see image for location		
54.72	42.48	bd	2.89	0.31	0.07	99.25	04-5-2 Grain #3 (see image for location		
54.91	42.24	bd	3.22	0.17	0.05	99.23	04-5-2 Grain #3 (see image for location		
55.01	41.51	0.006	2.95	0.11	bd	98.35	04-5-2 Grain #3 (see image for location		
55.36	41.77	bd	2.82	0.37	0.05	99.18	04-5-2 Grain#4 (see image) Small adj Mn		
55.92	43.12	0.004	3.12	0.32	0.07	101.23	04-5-2 Grain#4 (see image) Small adj Mn		
54.46	42.10	bd	3.63	0.04	bd	98.71	04-5-2 Grain#4 (see image) in Plag		
54.10	41.73	0.008	3.34	0.11	bd	99.29	GR-05-1 Grain #1 core	bt, qtz, plag	
54.40	41.31	bd	3.34	0.05	bd	99.10	GR-05-1 Grain #1 core	bt, qtz, plag	
53.28	41.95	bd	2.59	0.10	0.05	97.97	GR-05-1 Grain #2 Core	bt, qtz, plag	
52.92	42.35	0.005	2.52	0.06	0.05	97.91	GR-05-1 Grain #2 Core	bt, qtz, plag	
52.69	42.23	0.005	2.63	bd	0.07	97.62	GR-05-1 Grain #3 core	bt, qtz, plag	
52.82	42.04	0.003	2.67	0.04	bd	97.58	GR-05-1 Grain #3 core	bt, qtz, plag	
53.24	42.06	0.005	2.50	0.11	0.06	97.98	GR-05-1 Grain #13 core	qtz, bt	
53.43	41.90	bd	2.97	0.06	0.06	98.41	GR-05-1 Grain #9 core	bt, qtz, plag	
53.48	41.78	0.007	3.11	bd	bd	98.38	GR-05-1 Grain #9 core	bt, qtz, plag	
53.84	41.15	0.015	2.72	0.20	bd	97.92	GR-05-2 Grain #16 Core in grt	gt	
53.94	42.02	0.006	2.62	0.11	0.05	98.74	GR-05-2 Grain #17 core	bt, qtz	
53.92	41.75	0.011	2.89	0.04	0.05	98.65	GR-05-2 Grain #17 rim	bt, qtz	
53.31	41.80	0.009	2.50	0.07	0.05	97.75	GR-05-2 Grain #17B (Adj Grt) Core	bt, qtz, gt	
55.00	41.51	0.006	3.51	0.07	bd	100.10	GR-05-2 Grain #9 Core	bt, qtz, plag	
54.12	41.29	0.007	2.87	0.09	0.03	98.40	GR-05-2 Grain #9 Core	bt, qtz, plag	
54.63	41.83	0.008	2.69	0.08	0.07	99.31	GR-05-2 Grain #5 core	bt, qtz, plag	
54.53	41.62	0.005	2.59	bd	0.03	98.78	GR-05-2 Grain #5 core	bt, qtz, plag	
							INCOPE		
53.08	42.50	0.153	2.34	bd	0.09	98.42	GR-05-03 (Grain #1) in Grt	gt	core
53.93	42.19	0.143	2.32	0.05	bd	98.63	GR-05-03 (Grain #1) in Grt	gt	core
53.60	42.32	0.147	2.35	0.03	0.06	98.70	GR-05-03 (Grain #1) in Grt	gt	core
53.45	41.85	0.135	2.43	bd	bd	97.87	GR-05-03 (Grain #1) in Grt	gt	core
53.87	41.81	0.157	2.39	bd	0.07	98.45	GR-05-03 (Grain #1) in Grt	gt	core
54.52	42.13	0.013	2.96	bd	0.12	99.87	GR-05-03 (Grain #2) Grt Edge	gt	rim, bt
54.58	42.45	0.016	2.95	bd	0.07	100.09	GR-05-03 (Grain #2) Grt Edge	gt	ribt

CaO	P2O5	Cl	F	FeO	MnO	total	Comment	phase	
wt %	wt %	wt %	wt %	wt %	wt %	wt %			
54.40	41.82	0.019	3.41	bd	bd	99.69	GR-05-03 (Grain #2) Grt Edge	gt	rim, bt
54.34	42.11	0.015	2.59	bd	0.04	99.27	GR-05-03 (Grain #2) Grt Edge	gt	rim, bt
53.32	41.90	0.008	2.76	bd	bd	98.11	GR-05-03 (Grain #3)	bt	
54.17	41.94	0.020	2.75	bd	bd	98.96	GR-05-03 (Grain #3)	bt	
54.20	41.88	0.018	2.37	bd	bd	98.59	GR-05-03 (Grain #3)	bt	
53.92	41.84	0.013	2.60	0.07	bd	98.50	GR-05-03 (Grain #3)	bt	
53.83	41.61	0.012	2.78	bd	bd	98.37	GR-05-03 (Grain #3)	bt	
53.09	41.44	0.015	2.43	bd	0.05	97.15	GR-05-03 (Grain #4)	bt, qtz	
53.76	42.22	0.013	2.51	bd	bd	98.63	GR-05-03 (Grain #4)	bt, qtz	
53.56	42.34	0.006	2.44	0.04	bd	98.49	GR-05-03 (Grain #4)	bt, qtz	
54.87	42.08	0.019	2.90	bd	0.05	100.16	GR-05-03 (Grain #5)	bt, musc	
54.66	41.74	0.015	3.45	0.03	bd	99.92	GR-05-03 (Grain #5)	bt, musc	
54.70	41.32	0.017	3.41	bd	bd	99.51	GR-05-03 (Grain #5)	bt, musc	
54.87	42.07	0.019	3.31	0.03	0.04	100.37	GR-05-03 (Grain #6)	bt, qtz	
54.35	41.45	0.010	3.23	0.03	bd	99.38	GR-05-03 (Grain #6)	bt, qtz	
54.37	41.56	0.014	3.43	bd	bd	99.50	GR-05-03 (Grain #6)	bt, qtz	
53.30	42.48	0.014	2.46	bd	0.08	98.57	GR-05-04B (Grain #1)	bt, qtz	
53.40	41.34	0.011	2.37	bd	0.05	97.40	GR-05-04B (Grain #1)	bt, qtz	
53.08	41.98	0.010	2.31	0.05	0.11	97.74	GR-05-04B (Grain #1)	bt, qtz	
53.25	42.03	0.012	2.39	bd	0.03	97.97	GR-05-04B (Grain #1)	bt, qtz	
53.50	42.34	0.011	2.47	bd	0.04	98.39	GR-05-04B (Grain #1)	bt, qtz	
53.83	42.13	0.016	2.63	0.05	0.03	98.71	GR-05-04B (Grain #1)	bt, qtz	
56.19	43.07	0.011	3.14	bd	bd	102.44	GR-05-04B (Grain #2)	bt, qtz	
55.33	41.51	0.011	3.14	bd	0.08	100.23	GR-05-04B (Grain #2)	bt, qtz	
54.74	41.38	0.015	2.99	bd	0.04	99.20	GR-05-04B (Grain #2)	bt, qtz	
54.88	42.26	0.015	3.13	bd	0.07	100.51	GR-05-04B (Grain #2)	bt, qtz	
54.90	42.51	0.011	2.66	0.05	bd	100.19	GR-05-04B (Grain #3)	bt, qtz	
54.58	41.56	0.008	3.20	bd	bd	99.58	GR-05-04B (Grain #3)	bt, qtz	
55.18	42.47	0.010	3.14	bd	0.06	101.00	GR-05-04B (Grain #3)	bt, qtz	
55.15	42.02	0.008	3.27	0.03	0.07	100.70	GR-05-04B (Grain #3)	bt, qtz	
54.27	42.67	0.010	2.61	bd	0.05	99.87	GR-05-04B (Grain #4)	bt, qtz	
54.44	42.22	0.014	3.35	bd	0.05	100.15	GR-05-04B (Grain #4)	bt, qtz	
54.41	42.00	0.004	3.54	bd	bd	100.10	GR-05-04B (Grain #4)	bt, qtz	
53.45	42.55	0.011	1.94	0.05	bd	98.10	GR-05-04A (Grain #1) in Grt	gt	core
52.86	42.15	0.011	1.96	bd	bd	97.00	GR-05-04A (Grain #1) in Grt	gt	core
53.23	41.88	0.018	1.94	bd	0.04	97.26	GR-05-04A (Grain #1) in Grt	gt	core

CaO	P2O5	Cl	F	FeO	MnO	total	Comment	phase	
wt %	wt %	wt %	wt %	wt %	wt %	wt %			
54.11	42.94	0.006	2.02	bd	bd	99.08	GR-05-04A (Grain #1) in Grt	gt	core
54.57	41.96	0.026	2.48	bd	0.03	99.22	GR-05-04A (Grain #2) in Grt	gt	core
54.47	42.00	0.023	2.48	0.03	bd	99.06	GR-05-04A (Grain #2) in Grt	gt	core
54.58	42.06	0.008	2.29	bd	0.07	99.14	GR-05-04A (Grain #2) in Grt	gt	core
54.05	42.05	0.007	2.72	bd	0.06	99.07	GR-05-04A (Grain #3)	bt, qtz	
54.30	42.01	0.013	3.50	bd	0.07	99.91	GR-05-04A (Grain #3)	bt, qtz	
54.61	41.68	0.013	3.40	bd	bd	99.97	GR-05-04A (Grain #3)	bt, qtz	
54.41	42.05	0.014	3.60	0.04	0.04	100.25	GR-05-04A (Grain #3)	bt, qtz	
54.68	42.85	0.013	2.64	bd	0.06	100.29	GR-05-04A (Grain #4)	bt, qtz	
54.21	42.60	0.006	2.62	bd	0.04	99.47	GR-05-04A (Grain #4)	bt, qtz	
54.17	42.23	0.007	3.18	bd	0.05	99.65	GR-05-04A (Grain #4)	bt, qtz	
54.57	42.60	0.006	2.68	bd	bd	99.88	GR-05-04A (Grain #4)	bt, qtz	
53.41	42.46	0.008	3.13	0.06	0.04	99.18	GR-05-04A (Grain #4)	bt, qtz	
53.40	42.55	0.010	2.50	0.05	bd	98.66	GR-05-04A (Grain #5)	bt, qtz	
53.72	42.30	0.012	2.61	0.04	0.03	98.85	GR-05-04A (Grain #5)	bt, qtz	
54.29	42.76	0.010	2.69	0.03	0.10	99.97	GR-05-04A (Grain #5)	bt, qtz	
53.54	42.01	0.010	2.65	0.04	bd	98.32	GR-05-04A (Grain #5)	bt, qtz	
53.74	42.33	0.011	2.66	bd	0.03	99.06	GR-05-04A (Grain #5)	bt, qtz	
53.20	41.88	0.010	2.56	bd	0.09	97.75	GR-05-04A (Grain #6)	bt, qtz	
54.15	42.64	0.013	2.44	0.04	0.06	99.60	GR-05-04A (Grain #6)	bt, qtz	
53.56	41.90	0.008	2.41	bd	0.11	98.16	GR-05-04A (Grain #6)	bt, qtz	
54.28	42.72	0.008	2.43	bd	0.10	99.72	GR-05-04A (Grain #6)	bt, qtz	
52.83	41.90	0.014	2.37	bd	0.08	97.32	GR-05-04A (Grain #6)	bt, qtz	
53.60	41.93	0.011	2.34	bd	0.12	98.24	GR-05-04A (Grain #6)	bt, qtz	
55.03	41.90	0.009	3.34	0.04	bd	100.35	GR-05-4A Grain #13 Core	bt, qtz	
54.67	41.34	0.009	3.16	0.10	0.05	99.32	GR-05-4A Grain #13 Core	bt, qtz	
54.83	41.85	0.006	3.35	0.06	0.07	100.15	GR-05-4A Grain #13 rim	bt, qtz	
55.07	41.75	0.014	3.31	0.03	0.09	100.28	GR-05-4A Grain #13B (in green) rim	bt, qtz	
55.07	41.52	0.011	2.90	0.13	bd	99.64	GR-05-4A Grain #13B (in green) rim	bt, qtz	
54.74	41.61	0.008	3.23	0.10	0.04	99.72	GR-05-4A Grain #17 core	gt	
54.90	41.85	0.008	2.45	0.03	0.05	99.28	GR-05-4A Grain #17 core	gt	
54.94	40.51	0.017	3.21	0.19	bd	98.88	GR-05-4A Grain #17 rim	gt	
54.70	41.80	0.010	3.37	0.05	bd	99.93	Line 1 GR-05-04A Trav Grain 64um spacin	gt	
55.60	42.01	0.010	3.18	0.06	0.06	100.92	Line 2 GR-05-04A Trav Grain 64um spacin	gt	
54.51	42.00	0.015	2.47	0.04	0.10	99.13	Line 3 GR-05-04A Trav Grain 64um spacin	gt	
55.18	41.56	0.011	3.28	0.14	0.03	100.20	Line 4 GR-05-04A Trav Grain 64um spacin	gt	

CaO	P2O5	Cl	F	FeO	MnO	total	Comment	phase	
wt %	wt %	wt %	wt %	wt %	wt %	wt %			
55.40	42.07	0.014	2.59	0.09	0.04	100.20	Line 5 GR-05-04A Trav Grain 64um spacin	gt	
55.42	41.96	0.006	2.62	0.10	bd	100.12	GR-05-4A Grain #7 Core	gt	
55.17	41.94	0.012	3.24	0.08	0.07	100.51	GR-05-4A Grain #7 Core	gt	
55.44	41.28	0.010	2.99	bd	0.05	99.77	GR-05-4A Grain #6 core	bt, qtz	
55.65	41.66	0.008	2.98	0.11	bd	100.42	GR-05-4A Grain #6 core	bt, qtz	
54.98	41.08	0.011	2.35	0.11	bd	98.53	GR-05-4A Grain #4 Core	bt, qtz, plag	
55.40	41.93	0.012	2.84	0.03	0.07	100.28	GR-05-4A Grain #4 rim	bt, qtz, plag	
55.27	42.12	0.010	2.73	0.09	bd	100.23	GR-05-4A Grain #4B		
54.67	41.64	0.020	2.86	0.07	bd	99.28	GR-05-4A Grain #4B		
55.37	42.00	0.008	2.96	0.15	bd	100.50	GR-05-4A Grain #4B rim		
55.35	42.80	0.013	2.86	0.94	bd	100.78	04-5-5 Grain#1 (In Grt)	gt	
54.98	41.63	0.003	2.77	0.69	bd	98.90	04-5-5 Grain#2 (In Grt)	gt	
53.38	41.11	0.008	2.79	0.07	0.04	96.22	04-5-5 Grain#3 Rim		
53.65	41.23	0.007	2.84	0.11	0.05	96.69	04-5-5 Grain#3 Core		
54.34	41.62	0.006	3.01	bd	bd	97.71	04-5-5 Grain#3 Core		
54.72	42.11	0.008	3.05	0.07	0.06	98.74	04-5-5 Grain#3 Rim		
53.64	41.23	0.020	2.51	bd	0.04	96.38	04-5-5 Grain#4 Rim		
53.38	41.20	0.034	2.95	0.10	bd	96.42	04-5-5 Grain#4 Core		
53.93	41.76	0.008	2.71	0.04	0.04	97.34	04-5-5 Grain#4 Core		
54.04	42.12	0.014	2.80	0.10	0.04	97.93	04-5-5 Grain#4 Rim		
53.39	41.32	0.012	2.68	0.39	bd	96.67	04-5-5 Grain#5 Rim		
54.14	42.01	0.018	2.89	0.43	0.07	98.34	04-5-5 Grain#5 Core		
55.10	42.49	0.012	2.76	0.54	bd	99.73	04-5-5 Grain#5 Core		
54.11	42.20	0.019	2.54	0.71	0.03	98.52	04-5-5 Grain#6 Small Grain		
54.66	40.92	0.019	2.93	0.34	0.05	97.69	04-5-5 Grain#7		
54.38	41.46	0.016	2.80	0.21	bd	97.67	04-5-5 Grain#7		
54.70	41.79	0.015	3.43	0.50	bd	99.00	04-5-5 Grain#8 Rim		
54.55	42.04	0.026	3.13	0.37	0.04	98.84	04-5-5 Grain#8 Core		
54.71	41.81	0.006	3.09	0.40	0.03	98.75	04-5-5 Grain#8 Core		
54.86	41.83	0.050	2.71	0.71	0.07	99.08	04-5-5 Grain#9		
54.11	42.10	0.047	2.76	0.62	bd	98.48	04-5-5 Grain#9		
55.04	43.06	0.009	3.97	0.14	0.06	100.61	04-5-5 Grain#10 adj leucosome		
54.62	41.95	bd	3.73	0.17	0.04	98.94	04-5-5 Grain#10 adj leucosome (core)		

CaO	P2O5	Cl	F	FeO	MnO	total	Comment	phase	
wt %	wt %	wt %	wt %	wt %	wt %	wt %			
54.87	42.35	0.004	3.92	0.05	bd	99.54	04-5-5 Grain#10 adj leucosome (core)		
54.50	42.36	0.006	3.45	0.09	0.04	98.99	04-5-5 Grain#10 adj leucosome (rim)		
54.40	41.60	0.006	2.98	0.22	0.04	97.99	04-5-5 Grain#11 (rim)		
53.11	40.63	0.016	3.00	0.04	bd	95.55	04-5-5 Grain#11 (core)		
54.25	42.02	0.008	3.11	0.01	0.04	98.13	04-5-5 Grain#11 (rim)		
54.87	41.76	bd	3.41	0.13	0.03	98.77	04-5-5 Grain#12 Rim		
54.90	41.98	0.006	3.10	bd	bd	98.69	04-5-5 Grain#12 Core		
54.82	42.24	0.009	3.39	bd	bd	99.04	04-5-5 Grain#12 Core		
54.60	41.88	0.003	3.10	0.05	0.09	98.42	04-5-5 Grain#12 Rim		
54.64	41.87	0.010	3.55	0.11	bd	98.68	04-5-5 Grain#12 Rim		
54.55	42.05	0.008	3.27	0.11	bd	98.60	04-5-5 Grain#12 Rim		
54.32	42.01	0.011	2.83	bd	bd	97.97	04-5-5 Grain#13 Traverse		
54.35	42.06	0.011	2.97	bd	0.06	98.19	04-5-5 Grain#13 Traverse		
54.18	41.77	0.010	2.93	0.03	bd	97.69	04-5-5 Grain#13 Traverse		
53.79	41.94	0.013	2.90	bd	bd	97.43	04-5-5 Grain#13 Traverse		
54.92	41.69	bd	2.93	0.21	bd	98.52	04-5-5 Grain#13 Traverse		
CaO	**P2O5**	**Cl**	**F**	**FeO**	**MnO**	**total**			
							Abandoned	average ap	
54.24	42.05	0.008	2.92	0.19	0.05	99.05			
0.87	0.43	0.004	0.29	0.20	0.02	1.03			
							INCOPE	average ap	
54.64	41.79	0.013	3.02	0.20	0.05	98.84			
0.58	0.45	0.009	0.34	0.22	0.02	1.24			
							Abandoned	in gt	
55.11	42.37	0.011	2.83	0.49	0.05	99.81	mean		
0.76	0.68	0.004	0.35	0.17	0.02	1.21	stdev (1 sigma)		
							INCOPE	in gt	
54.43	42.02	0.037	2.65	0.17	0.06	99.23	mean		
0.75	0.45	0.053	0.46	0.26	0.03	0.98	stdev (1 sigma)		
							Abandoned	bordering bt, qtz, plag	
53.58	41.82	0.007	2.83	0.07	0.05	98.32	mean		
0.77	0.31	0.003	0.32	0.03	0.01	0.81	stdev (1sigma)		
							INCOPE	bordering bt, qtz, plag	
54.90	42.12	0.009	3.38	0.10	0.05	99.48	mean		
0.32	0.66	0.004	0.65	0.06	0.02	0.82	stdev (1sigma)		

CaO	P2O5	Cl	F	FeO	MnO	total			
wt %	wt %	wt %	wt %	wt %	wt %	wt %	Abandoned		
54.08	42.05	0.007	2.98	0.06	0.05	99.28	mean	bordering bt, qtz	
0.63	0.36	0.002	0.26	0.04	0.01	0.98	stdev (1 sigma)		
							INCOPE		
54.26	42.08	0.011	2.87	0.05	0.06	99.39	mean	bordering bt, qtz	
0.75	0.45	0.003	0.39	0.03	0.03	1.05	stdev (1 sigma)		

Table 1: EPMA results for analysis points with apatite in samples 04-5-2, GR-5-1, GR-5-2 (Abandoned quarry) and 04-5-5, GR-5-3, GR-5-4A, GR-5-4B (INCOPE quarry).

Bt = biotite
Qtz = quartz
Plag = plagioclase
Gt = garnet
Musc = muscovite
Ap = apatite

Minimum detection limits (ppm)	
Ca	50
P	200
Cl	28
F	226
Fe	300
Mn	250

Uncertainty in counting	
F	1%
Cl	15%

EPMA settings	
Accelerating voltage	15 kV
Cup current	10 nA
Beam diameter	5 μm